JOURNAL OF MATERIALS SCIENCE **30** (1995) 5146–5150

Study of the reaction of lanthanum nitrate with metal oxides present in the scale formed at high temperatures on stainless steel

M. I. RUIZ, A. HEREDIA, J. BOTELLA
Acerinox, S. A. Los Barrios, Cádiz, Spain
J. A. ODRIOZOLA*
Departamento de Química Inorgánica e Instituto de Ciencia de Materiales, Universidad de Sevilla-CSIC, Apartado 874 E-41080 Sevilla, Spain

The reaction of lanthanum nitrate with metallic oxides that can be present in the oxide scales formed at elevated temperatures on the surface of stainless steel has been investigated as model systems of the processes occurring during the oxidation of lanthanum coated stainless steel. X-ray diffraction (XRD) experiments have shown that $LaCrO_3$ and $LaFeO_3$ are the most stable compounds. XRD, chemical analysis and thermogravimetric experiments have demonstrated that in the case of Cr_2O_3, nitrate anions are able to oxidize Cr(III) to Cr(VI) resulting in a precursor phase of perovskite structure that influences the corrosion inhibition of stainless steel at high temperatures.

1. Introduction

Heat-resisting alloys depend on the formation of a protective oxide on the metal surface to limit section loss by oxidation. Generally, this protective oxide is chromia, Cr_2O_3 [1]. Approximately 50 years ago, it was discovered that minor amounts of reactive elements, added as a cerium mischmetall deoxidizer to the melt before the development of vacuum melting, greatly affected the lifetime of heater alloys [2]. This effect is called nowadays the "reactive element effect" (REE) [3].

The full manifestation of the effect can be produced by many elements, and by fine dispersions of the oxides of the reactive elements in the alloy [4, 5]. At least part of the effects can be produced by implanting the reactive element into the surface of the alloy [6–8], or by coating the surface with a thin layer of the reactive element oxide [9–13].

Despite the numerous efforts devoted to understanding the effect of rare-earth elements in the oxidation mechanism within the oxide scale, no clear conclusions have yet been drawn. The modification of the diffusivity in grain boundaries or of oxide scale morphology and grain size and change in the protective scale transport properties, might justify the beneficial effect of rare-earth cations [3].

In a recent report we postulated the formation of a perovskite compound, $LaCrO_3$, as responsible for the modification of the transport properties within the oxide scale [13]. This hypothesis slightly modifies previous data in which, although considering the presence of the perovskite phase, it is concluded that $LaCrO_3$ phases do not affect the corrosion behaviour [7, 8]. More recently, Roy *et al.* [14] observe a X-ray diffraction differences in the phases formed on oxidizing a CeO_2-coated stainless steel.

In the present report we present a systematic study of the phases formed on heating lanthanum nitrate with mixtures of oxides that can be present in the oxide scale of an oxidized stainless steel

2. Experimental procedure

Cr_2O_3 and Fe_2O_3 of 99% and 95% purity, NiO of 70% Ni content from Merck, MnO and $MnCr_2O_4$ 99% pure from Alpha products, were used as starting materials. A 1 M solution of $La(NO_3)_3 \cdot 6H_2O$ (Merck, 99% pure) in ethanol was prepared and mixed in adequate amounts with the pure oxides, simulating in this way the deposition process followed in the preparation of the coated steels [13]. The reacted specimens were obtained by the ceramic method by heating in an electric furnace up to 500, 900 or 1100 °C and keeping an isothermal step of 10 min at every temperature.

X-ray diffraction experiments were carried out on powdered samples in a Siemens Kristalloflex D5000 using Cu$K\alpha$ radiation and graphite as monochromator. Thermogravimetric measurements were performed in a Setaram TAG 24S16 device in synthetic air at $\beta = 10\,\mathrm{K\,min^{-1}}$.

---

*Author to whom all correspondence should be addressed.

0022–2461 © *1995 Chapman & Hall*

3. Results and discussion

The oxide scale of an AISI304 stainless steel after time-controlled oxidation at 900 °C under synthetic air is formed by Cr_2O_3 and $MnCr_2O_4$ [13, 15]. After depositing lanthanum, the presence of $LaCrO_3$ is also observed. A series of mixed oxides containing iron, chromium and manganese can be present depending on the degree of lanthanum coverage and the oxidation temperature [13]. By mixing the pure oxides with lanthanum nitrate we have attempted to understand the differences in the crystalline phases formed during oxidation on the surface of stainless steel.

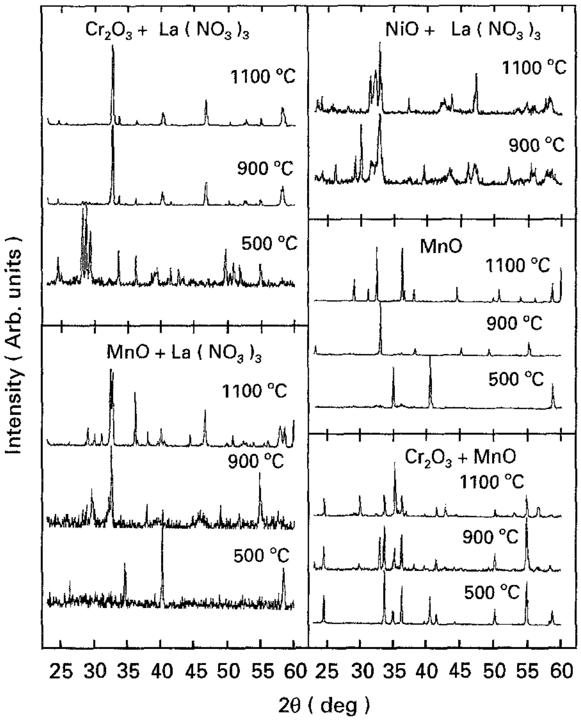

Figure 1 X-ray diffraction patterns of the resulting products after heating chromium, manganese and nickel oxide with lanthanum nitrate at the indicated temperatures. For the sake of comparison, the XRD patterns of the products resulting from heating MnO and Cr_2O_3 and MnO mixtures are also included

Fig. 1 presents the XRD patterns of binary mixtures of chromium, nickel and manganese oxides heated in air in the presence of lanthanum nitrate at 500, 900 and 1100 °C, all the crystalline phases observed are shown in Table I. For the sake of comparison, in the case of manganese oxide, MnO, the thermal evolution of the XRD pattern is also shown. In general, on heating these binary mixtures to the higher temperature used, mixed oxides of lanthanum and the transition metal are observed, although sometimes the observed phase is not the stoichiometric one. In particular, La–Ni compounds show a high compositional variability at high temperature, as can be expected because the following processes occur at 1100 °C: $LaNiO_3 \rightarrow La_4Ni_3O_{10} \rightarrow La_3Ni_2O_7$.

Ternary mixtures have been also investigated. Fig. 2 shows the XRD patterns of these mixtures as a function of temperature, the observed phases being described in Table II. The reaction of Cr_2O_3 with NiO and $La(NO_3)_3$ results at high temperatures in $LaCrO_3$ and La_2NiO_4, although this latter compound can only be observed in minute amounts. Besides this, the enormous variability of La–Ni–O phases observed on heating the binary mixtures was not observed in the presence of chromium, indicating a higher stability of the La–Cr–O phases with respect to those containing nickel. If $MnCr_2O_4$ is mixed with lanthanum the final product is again the chromium lanthanum perovskite which results in displacing the manganese from the spinel structure. The reaction between chromium and iron oxides with $La(NO_3)_3$ results in a mixture of $LaCrO_3$ and $LaFeO_3$ although the presence of iron oxide in the final product may indicate a higher stability of the chromium perovskite.

TABLE I Observed phases in binary mixtures as a function of the reaction temperature. (tr) = trace

Binary Mixture	500 °C	900 °C	1100 °C
$Cr_2O_3 + La(NO_3)_3 \cdot 6H_2O$	Cr_2O_3 La_2CrO_6	Cr_2O_3 $LaCrO_3$ La_2CrO_6(tr)	Cr_2O_3 $LaCrO_3$
$NiO + La(NO_3)_3 \cdot 6H_2O$		NiO La_2O_3 $LaNiO_3$ La_2NiO_4	NiO (tr) La_2O_3 (tr) $LaNiO_3$ La_2NiO_4 $La_4Ni_3O_{10}$ $La_3Ni_2O_7$
$MnO + La(NO_3)_3 \cdot 6H_2O$	MnO Mn_2O_3 (tr) $LaMnO_3$ (tr)	MnO (tr) Mn_2O_3 La_2O_3 Mn_3O_4 (tr) $LaMnO_3$ (tr)	Mn_3O_4 La_2O_3 (tr) $LaMnO_{3.15}$
MnO	MnO Mn_2O_3 (tr) Mn_3O_4 (tr)	Mn_2O_3 Mn_3O_4 (tr)	Mn_3O_4
Cr_2O_3 + MnO	MnO Cr_2O_3	Cr_2O_3 Mn_2O_3 Mn_3O_4 (tr) $MnCr_2O_4$	Cr_2O_3 Mn_2O_3 (tr) $MnCr_2O_4$

Finally, the diffractograms obtained after reacting $La(NO_3)_3$ with Cr_2O_3, Fe_2O_3 and MnO are shown in Fig. 3. The behaviour is quite similar to that found in the ternary mixtures the presence of chromium perovskite and manganese and iron oxides being detectable. Fig. 3 also shows the diffractograms obtained after reaction of $MnCr_2O_4$, Fe_2O_3 and $La(NO_3)_3 \cdot 6H_2O$. In this case, both iron and chromium perovskites are formed. The observed phases for both reactions are shown in Table III. This behaviour again confirms the higher stability of the $LaCrO_3$ compound with respect to the other possible lanthanum mixed oxides.

Apart from the above, it is interesting to notice the existence of La_2CrO_6 whenever lanthanum and chromium are present. To ensure the presence of Cr(VI), chemical analysis of this phase has been performed. After reacting $La(NO_3)_3$ with Cr_2O_3 at 500 °C water is added to the final product; after 3 h the solution is titrated with $Fe(NH_4)_2(SO_4)_2$ and the amount of Cr(VI) evaluated. This analysis shows 1.14% of the total weight corresponds to chromium (VI), which is consistent with the presence of the La_2CrO_6 phase. To ensure that this is not due to oxidation by air, the same analysis was performed on pure Cr_2O_3 heated in air at 500 °C; in this case only 0.033% of the weight of the sample can be associated with chromium (VI). By mixing Cr_2O_3 and La_2O_3 and oxidizing in air at 500 °C, only 0.01% of the total Cr(III) is present as Cr(VI), while if $Al(NO_3)_3$ is added to the mixture, the amount of Cr(VI) in the solution increases to 0.46% of the total chromium content. Therefore, it should be stated that NO_3^- anions must oxidize Cr(III) to Cr(VI).

To understand the processes occurring in the oxide scale of stainless steel when $La(NO_3)_3$ is added, we have performed a thermogravimetric study of the reaction of Cr_2O_3 with $La(NO_3)_3$. Fig. 4 shows the

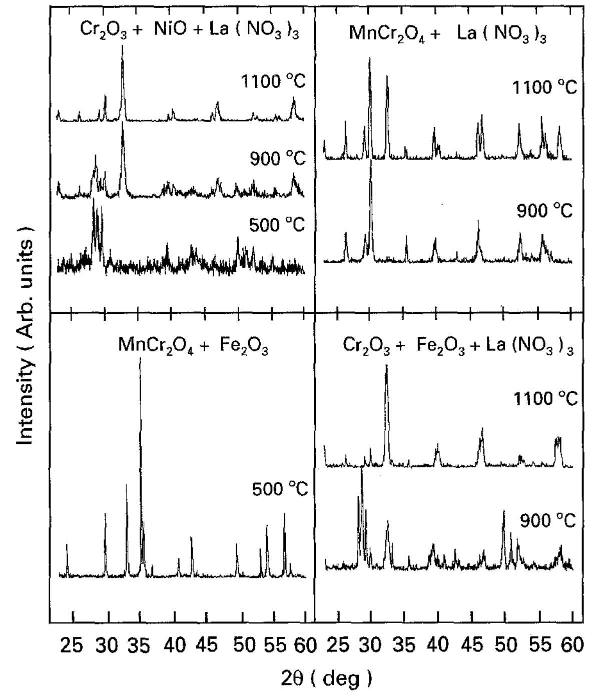

Figure 2 X-ray diffraction patterns of the resulting products after heating binary mixtures of metallic oxides with lanthanum nitrate at the indicated temperatures. For the sake of comparison, the XRD patterns of the products resulting from heating $MnCr_2O_4$ and Fe_2O_3 and MnO mixtures are also included

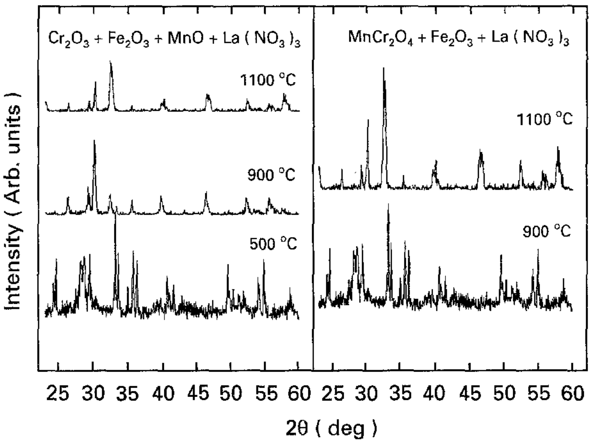

Figure 3 X-ray diffraction patterns of the resulting products after heating Cr_2O_3, Fe_2O_3 and MnO or $MnCr_2O_4$ and Fe_2O_3 with lanthanum nitrate at the indicated temperatures.

TABLE II Observed phases in ternary mixtures as a function of the reaction temperature. (tr) = trace

Ternary mixture	500 °C	900 °C	1100 °C
$Cr_2O_3 + NiO + La(NO_3)_3 \cdot 6H_2O$	Cr_2O_3 NiO (tr) La_2CrO_6	Cr_2O_3 $LaCrO_3$ La_2CrO_6 NiO (tr) $LaNiO_3$	NiO (tr) La_2O_3 $LaCrO_3$ La_2NiO_4 (tr)
$MnCr_2O_4 + La(NO_3)_3 \cdot 6H_2O$	No reaction	La_2O_3 $MnCr_2O_4$	La_2O_3 $LaCrO_3$ $MnCr_2O_4$
$MnCr_2O_4 + Fe_2O_3$	$MnCr_2O_4$ Fe_2O_3 $MnFe_2O_4$ (tr)	No further reaction	
$Cr_2O_3 + Fe_2O_3 + La(NO_3)_3 \cdot 6H_2O$		$LaCrO_3$ La_2CrO_6 La_2O_3 $FeLaO_3$ Fe_2O_3	$LaCrO_3$ La_2O_3 $LaFeO_3$

TABLE III Observed phases in quaternary mixtures as a function of the reaction temperature. (tr) = trace

Quaternary mixture	500 °C	900 °C	1100 °C
$Cr_2O_3 + Fe_2O_3 + MnO + La(NO_3)_3 \cdot 6H_2O$	Cr_2O_3 Fe_2O_3 MnO La_2CrO_6	Cr_2O_3 Fe_2O_3 Mn_2O_3 $LaCrO_3$	Cr_2O_3 Fe_2O_3 Mn_3O_4 $LaCrO_3$
$MnCr_2O_4 + Fe_2O_3 + La(NO_3)_3 \cdot 6H_2O$	–	Fe_2O_3 $LaFeO_3$ La_2O_3 $MnCr_2O_4$	$LaFeO_3$ $LaCrO_3$ La_2O_3 $MnCr_2O_4$

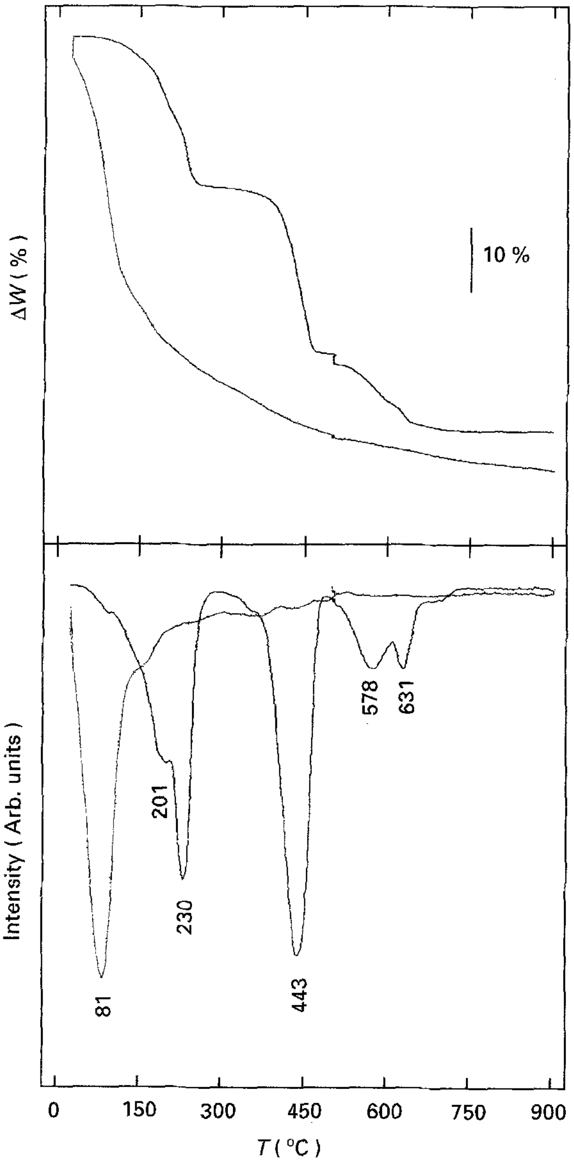

Figure 4 (a) Weight losses and (b) derivative weight losses of (···) Cr_2O_3 (a), (b) × 50, and (–) $La(NO_3)_3 \cdot 6H_2O$.

thermograms corresponding to the decomposition of the initial products in the presence of synthetic air. The thermal evolution of Cr_2O_3 presents a single step with the maximum rate at temperatures close to 100 °C indicative of the elimination of surface water corresponding to a highly sintered oxide. $La(NO_3)_3 \cdot 6H_2O$ is characterized by a more complex thermogram, having three main steps: between room temperature and 285 °C, the second one that extends up to 480 °C, and the last one at approximately 740 °C; the weight losses associated with these three steps are 23.9%, 25.9% and 12.2%, respectively. The first step and the third one are complex as deduced from the DTG being composed of more than one step. According to literature results, these steps can be associated with the loss of water, elimination of some of the nitrate groups through the formation of nitrogen oxides, resulting in the formation of oxynitrate phases as previously described for this and other systems [16, 17], and a final step to the formation of La_2O_3. Assuming the following decomposition scheme, $La(NO_3)_3 \cdot 6H_2O \rightarrow La(NO_3)_3 \rightarrow LaONO_3 \rightarrow La_2O_3$, the calculated weight losses for the three steps would be 24.9%, 25.0% and 12.5% respectively, in excellent agreement with the experimental results. The last step is clearly differentiated into two processes in the thermogram has weight losses that can be fitted to the process $LaONO_3 \rightarrow La_3O_4NO_3 \rightarrow La_2O_3$.

The thermogram of a mixture of Cr_2O_3 and $La(NO_3)_3 \cdot 6H_2O$ is shown in Fig. 5. Most of the weight loss occurs in two main steps at temperatures below 500 °C, these two steps are similar to those corresponding to the thermal decomposition of $La(NO_3)_3 \cdot 6H_2O$ and occurs in the same temperature range except the last shoulder in the DTG at 500 °C which appears in this case and not at all in the nitrate. When the amount lost up to 500 °C is analysed, the total weight loss (52.1%) is higher than that corresponding to the elimination of two nitrate ions (46.5%) but smaller than that corresponding to the total decomposition of nitrates (58.0%). It can be assumed that the decomposition occurs up to the formation of the final oxynitrate, $La_3O_4NO_3$, in which case, if the oxidation of Cr(III) to Cr(VI) occurs by the nitrate as stated above, resulting in the formation of the La_2CrO_6 phase, the observed weight loss has to be 51.9%, in excellent agreement with the experimental data. At higher temperatures, two decomposition steps appear that correspond to the elimination of molecular oxygen and to the elimination of the remaining nitrate groups with weight losses of 1.3% and 1.6%, respectively. As can be seen in Fig. 1 at 500 °C, the La_2CrO_6 phase is formed, decomposing at higher temperatures, resulting in the formation of the perovskite phase with the loss of the excess oxygen.

By depositing lanthanum nitrate over time-controlled preoxidized stainless steel surfaces, which consist of a layer of thickness between 0.1 and 0.2 μm of Cr_2O_3, the formation of $LaCrO_3$ is observed [13, 15]. This latter phase controls the diffusion of cations and

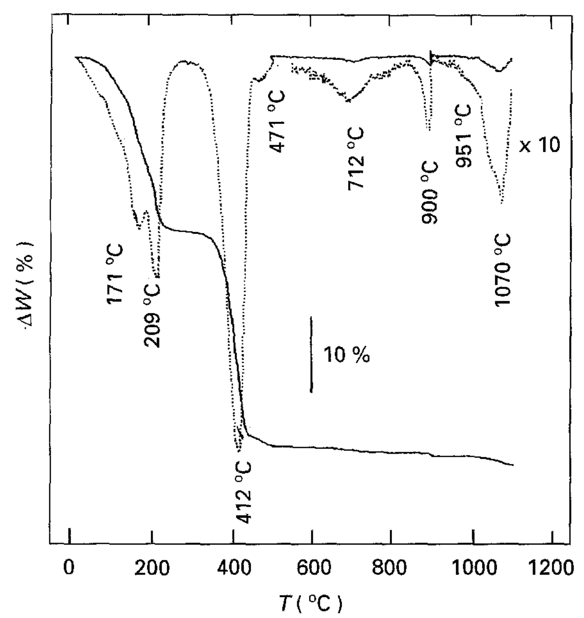

Figure 5 (—) Weight loss and (···) derivative weight loss of a 1:2 M mixture of Cr_2O_3 and $La(NO_3)_3 \cdot 6H_2O$.

therefore the oxidation kinetics. In a first step, the diffusion of anions generates a thick Cr_2O_3 layer, thickening towards the alloy–oxide–scale interface, up to the point at which the chromium diffusion from the alloy bulk and the thickness of the chromium oxide layer favours cationic diffusion. When this step takes place a layer of small $MnCr_2O_4$ crystals starts to grow on top of the perovskite layer. As small and stoichiometric as the lanthanum content is it is over the minimum level able to form a continous perovskite layer; under this lanthanum level, poorly stoichiometric Mn-, Fe- and Ni–Cr spinel-like structures appear.

The absence of Ni–La and Fe–La mixed oxides can be understood because initially a Cr_2O_3 layer is formed over the preoxidized stainless steel surface. This also occurs if in the initial oxidation layer the Mn–Cr spinel is present; in this case the formation of $LaCrO_3$ is explained either by direct reaction with the chromium oxide or by displacing manganese from the spinel structure. If, on the contrary, lanthanum nitrate is directly deposited over non-oxidized stainless steel, $LaFeO_3$ and $La_2Ni_2O_5$ are observed in the XRD diffraction patterns. This can be explained by the combined oxidizing effect of nitrate anions and oxygen which may result in the formation from the very beginning of Fe(III), Ni(II) and Cr(III) species on the material surface.

In conclusion, the reported data help us to understand the variability of phases encountered on analysing the oxide scale grown on stainless steel as a consequence of the reactivity of Cr_2O_3 and La_2O_3 which favours the formation of this perovskite over iron or nickel ones. In addition, the oxidizing behaviour of nitrate anions that leads to the formation of La_2CrO_6 also helps in favouring the formation of the La–Cr perovskite.

Acknowledgements

This work was partially supported by Plan Nacional de Materiales of the Comision Interministerial de Ciencia y Tecnología. (MAT95-1093-CE)

References

1. R. A. RAPP, *Metall. Trans.* **15 A** (1984) 765.
2. L. B. PFEIL, *UK Pat. 574 088* (1947).
3. J. STRINGER, *Mater. Sci. Eng. A* **120** (1989) 129.
4. T. N. RHYS-JONES and H. J. GRABKE, *Mater. Sci. Technol.* **4** (1988) 446.
5. T. AMANO and A. ITOH, *Appl. Surf. Sci.* **60/61** (1992) 677.
6. C. M. COTELL, G. J. YUREK, R. J. HUSSEY, D. F. MITCHELL and M. J. GRAHAM, *J. Electrochem. Soc.* **134** (1987) 1871.
7. K. PRZYBYLSKI, A. J. GARRATT-REED and G. J. YUREK, *ibid.* **135** (1988) 509.
8. K. PRZYBYLSKI and G. J. YUREK, *ibid.* **135** (1988) 517.
9. M. LANDKOF, A. V. LEVY, D. H. BOONE, R. GRAY and E. YANIV, *Corrosion* **41** (1985) 344.
10. P. Y. HOU and J. STRINGER, *Mater. Sci. Eng.* **87** (1987) 295.
11. G. BONNET, J. P. LARPIN and J. C. COLSON, *Solid State Ionics* **51** (1992) 11.
12. H. KONNO, M. TOKITA, A. FURUSAKI and R. FURUICHI, *Electrochim. Acta* **37** (1992) 2421.
13. M. I. RUIZ, J. ALMAGRO, A. HEREDIA, J. BOTELLA, J. J. BENITEZ and J. A. ODRIOZOLA, in "International Conference on Processes and Materials Innovation. Stainless Steel 1993", Vol. 3, edited by W. Nicodemi (Associazione Italiana di Metalurgia, Milano, 1993) p.77.
14. S. K. ROY, S. SEAL, S. K. BOSE and M. CAILLET, *J. Mater. Sci. Lett.* **12** (1993) 249.
15. F. J. AGER, M. A. RESPALDIZA, J. C. SOARES, M. F. SILVA, J. BOTELLA, J. J. BENITEZ and J. A. ODRIOZOLA, *Acta Metall. Mater.* in the press.
16. B. WUNDERLICH, "Thermal Analysis" (Academic Press, New York, 1990) p.390.
17. R. ALVERO, J. A. ODRIOZOLA, J. M. TRILLO and S. BERNAL, *J. Chem. Soc. Dalton Trans.* (1984) 87.

Received 1 December 1994
and accepted 17 May 1995.